Radiation Physics and Chemistry 224 (2024) 112016

Contents lists available at ScienceDirect

Radiation Physics and Chemistry

journal homepage: www.elsevier.com/locate/radphyschem

Attenuation images of optical CT using Fricke xylenol orange gel for dose mapping in radiotherapy

P.V.S. Tavares *, R.E. Diniz, O. Rodrigues Jr., L.L. Campos

Ionizing Radiation Metrology Center, Energy and Nuclear Research Institute, Avenue Professor Lineu Prestes, 2242, São Paulo 05508-000, SP, Brazil

ARTICLE INFO

Handling Editor: Dr. Chris Chantler

Keywords:
3D dosimetry
Fricke gel
Optical CT

ABSTRACT

The Fricke gel dosimeter, a gel-based solution containing ferrous ions, can be used for three-dimensional dosimetry by adding xylenol orange to the solution. This changes the optical properties, affecting radiation absorption. These gel dosimeters are recommended for clinical use, and 3D dosimetry uses optical computed tomography (OCT) to analyze reconstructed images. Advancements in radiotherapy focus on accurate irradiation while reducing doses to nearby tissues. This study uses modified FXO gel for 3D dosimetry, utilizing non-toxic, easy-to-handle reagents and optical CT Vista 16 equipment. The experiment aims to characterize the system's practicality and evaluate the impact of lead filters on attenuation values. The study also examines trends in attenuation values for different thicknesses of lead shields, enhancing our understanding of the relationship between attenuation and dose using optical CT. To prevent artifacts, a modified FXO gel was created by introducing a variation of XO in the preparation. The ideal concentration of XO is 0.01 mM to prevent distortions within the dose range of 1 Gy–10 Gy. A calibration system using FXO gel can be developed by comparing the maximum irradiation dose with the attenuation observed in the gel. The modified gel showed a sensitivity of $5.5{\cdot}10^{-3} \pm 2.6{\cdot}10^{-4}$ cm^{-1}/Gy and a starting dose of 4.2 Gy. Two samples were tested using different configurations of lead filters, with the central holes showing dose peaks of 4.72 Gy, 4.57 Gy, and 4.32 Gy, respectively. The results suggest the feasibility of producing modified FXO gels for examination in optical CT systems and their potential application in radiotherapy systems. Future research is being conducted in clinical irradiation to facilitate comparison with system designs.

1. Introduction

The fundamental structure of the Fricke dosimeter contains an acidic solution containing ferrous ions (Fe^{2+}) that undergo oxidation to ferric ions (Fe^{3+}) when irradiated (Potetnya et al., 2021). The research group at Yale University discovered that gel-based solutions could be used for three-dimensional dosimetry. They realized that the concentration of ferric ions in the ferrous sulfate dosimeter, which was originally developed by Fricke and Morse, could be measured using nuclear magnetic resonance (NMR) relaxometry (Gore and Kang, 1984; Gambarini et al., 1994; Luciani et al., 1996).

By adding xylenol orange (XO) to the Fricke gel solution, the ligand forms a compound with the Fe^{3+} ions, causing changes in the optical properties that depend on the dose and specific wavelengths (Gupta et al., 1982). Optical absorption is directly proportional to radiation absorption, and preventing light scattering is crucial for solution assessment (Kelly et al., 1998). Fricke xylenol orange gel dosimeters (FXO gel dosimeters) are recommended for clinical use, especially when combined with a rapid optical readout after being irradiated (Bero et al., 1999). 3D dosimetry with gel dosimeters uses optical computed tomography (OCT) to analyze reconstructed images, providing attenuation values correlated with the deposited dose (Rousseau et al., 2022, 2023).

The charge-coupled device (CCD)-based optical computed tomography system, Vista 16, utilizes 2D projections to generate 3D maps of optical attenuation for objects located inside the scanner region (Doran et al., 2001). The reconstruction is performed using pictures acquired from the FXO gel prior to and following irradiation (Oldham et al., 2003). The process of capturing images involves using an LED light at a wavelength of 590 nm, which is specifically chosen for radiochromic dosimeters. This light is directed towards the solution within a revolving aquarium (Xu et al., 2004).

The advancements in radiotherapy techniques focus on achieving accurate irradiation of the target area while reducing the radiation dose

* Corresponding author.
E-mail address: paulo.tavares@ipen.br (P.V.S. Tavares).

https://doi.org/10.1016/j.radphyschem.2024.112016
Received 29 February 2024; Received in revised form 24 June 2024; Accepted 30 June 2024
Available online 1 July 2024

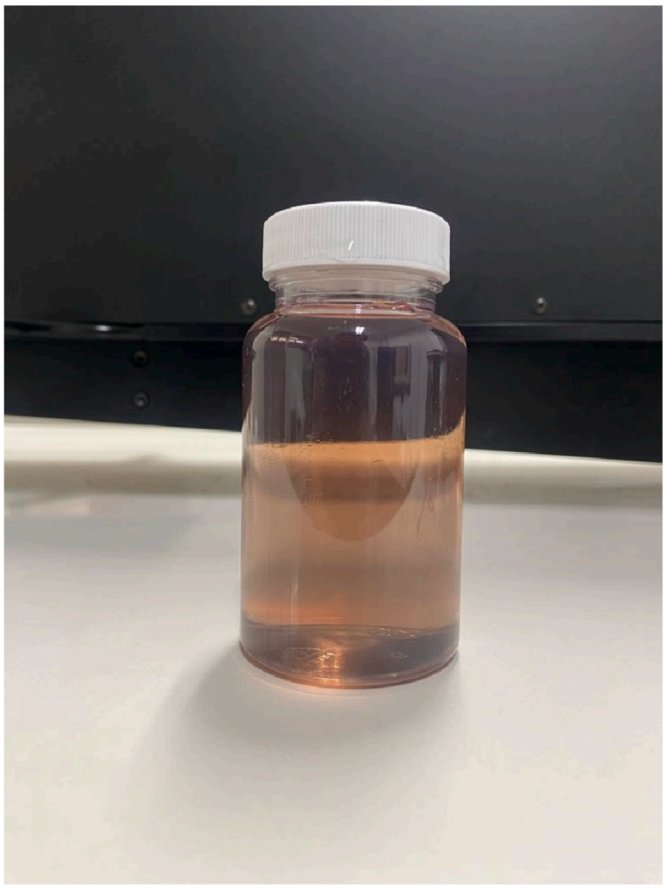

Fig. 1. Example of FXO gel in the flask used in Optical CT scanner.

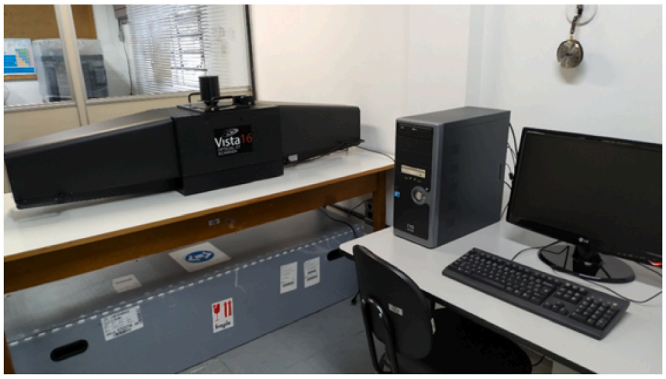

Fig. 2. Optical CT scanner Vista 16.

to nearby tissues in order to avoid potential problems that may result in treatment delays (Bolten et al., 2023). Intensity-modulated radiotherapy (IMRT), stereotactic radiosurgery, and stereotactic body radiotherapy (SBRT) use precise collimators to deliver correct doses of radiation to the tumor location using tiny photon fields. Nevertheless, the task of accuracy in the distribution of doses and the verification of dosimetry in these methods presents many obstacles, mainly because of the complications involved in experimental dosimetry for small fields (Azadeh et al., 2022; Höfel et al., 2023; Al Kafi et al., 2023).

The main objective of this study is to employ a methodology that utilizes the modified hydrogel FXO for the purpose of 3D dosimetry. The FXO for preparation uses non-toxic, easy-to-handle reagents that allow for modification of solutions for various applications, making the preparation process simple and effective (Del Lama et al., 2017; Liosi

Fig. 3. Gammacell 220 irradiator equipment.

et al., 2017; Babu S. et al., 2019). Optical CT Vista 16 is responsible for the reconstruction of images that correlate attenuation with dose (Woolvett and Jordan, 2023). The objective is to generate colormaps that represent attenuation by selecting slices from these reconstructed images.

The first stage of the experiment entailed characterizing the optical CT system to verify its practicality for utilization. Previous studies on the optical CT system have found artifacts caused by the solution's high attenuation value at the start, which makes the post-irradiation evaluation difficult. The cupping artifact, a specific artifact, is more commonly observed in radiochromic gels (Olding et al., 2009; Takanashi et al., 2019; Hayashi and Gotoh, 2020). The Gammacell system employs several Co-60 sources to carry out radio-sterilization, pest control, and simulate radiotherapy in small quantities (Colins et al., 2018; Mendes et al., 2020; Moradi et al., 2021). The system's suitability for characterization is attributed to its ability to emit isotropic radiation (Hefne, 2000; Rodrigues et al., 2010).

The FXO gel was irradiated in a system used to calibrate ionization cameras used in the field of radiotherapy. The system consists of a Theratron 780c irradiator and a water phantom with dimensions of 30 cm × 30 cm x 20 cm, in which the FXO gel is positioned. By utilizing the reconstruction image and the attenuation values, it is possible to construct a calibration curve that can be subsequently employed for examining other irradiations.

To evaluate the impact of lead filters on attenuation values, coronal slices along the X-axis and transverse slices along the Z-axis were implemented to evaluate the FXO hydrogel at various locations. The project aims to evaluate specific characteristics, including significant decreases in intensity observed at the center of lead shields, differences associated with varying thicknesses of lead shields, and the capability to identify perforations in lead shields.

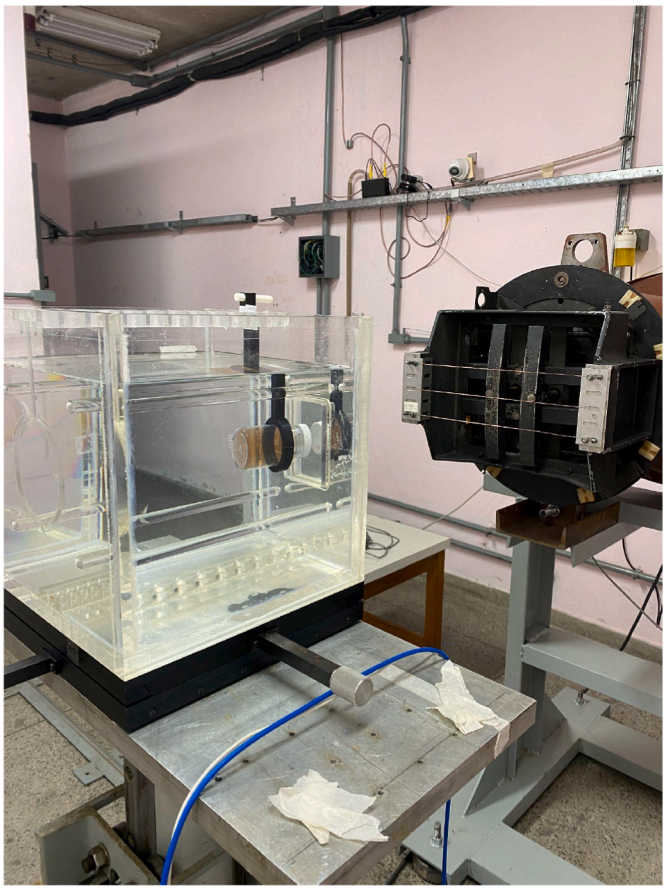

Fig. 4. Apparatus utilized for calibrating the FXO gel. The image shows the Theratron 780c equipment and the water phantom with the FXO gel.

Moreover, through the use of visual depictions, the objective is to examine and elucidate the trends in attenuation values for varying thicknesses of lead shields in different locations, specifically those with and without holes. This investigation is expected to enhance our understanding of the relationship between attenuation and dose by utilizing optical CT.

2. Methodology

2.1. Preparation of FXO gel and analysis in optical CT scanner Vista 16

To prepare the FXO gel, the following quantities of reagents were utilized: 5% bovine gelatin (270 Bloom, food grade from Gelita, Brazil); 50 mM of sulfuric acid (H_2SO_4), pro-analysis (PA) from Merck; 1 mM of sodium chloride (NaCl) pro-analysis (PA) from Merck; 1 mM of Mohr's salt/ferrous ammonium sulfate ($Fe(NH_4)_2(SO_4)_26H_2O$) pro-analysis (PA) from Merck; and various concentrations (0.1 mM, 0.05 mM, 0.03 mM, and 0.01 mM) of xylenol orange ($C_{31}H_{28}N_2Na_4O_{17}S$) pro-analysis (PA) from Merck.

It divides the initial solution into two portions, with one portion containing 25% of the total volume and the other portion containing 75% of the total volume, both of which are ultrapure water. Approximately 75% of ultrapure water is heated to a temperature of around 70 °C and subsequently combined with bovine gelatin. After mixing, the gelatin is allowed to cool to a temperature of 35 °C before being combined with the remaining 25% of ultrapure water and other reagents. The entirety of the gel is placed into a flask made of PETE material designed for use in the optical CT scanner Vista 16 (Fig. 1) and refrigerated (4 °C ± 1 °C) for 20 h until irradiation.

The optical CT Scanner Vista 16, shown in Fig. 2, does an analysis by scanning the gel both before and after irradiation. The VistaScan software is responsible for acquiring projections and performing reconstructions. Each analysis involves the acquisition of 500 image projections. The reconstruction is performed using the OSC-TV technique, as described in the prior studies (Matenine et al., 2015a, 2015b; Dekker et al., 2017).

2.2. Irradiations in the gammacell source

Initially, irradiation proceeded by utilizing four samples of FXO gel, each containing a distinct quantity of XO. The samples were irradiated with a dose of 10 Gy using the Gammacell equipment (Fig. 3). The reconstruction image of each sample was obtained, and the presence of the cupping artifact was evaluated. The sample that did not exhibit any artifacts in this phase was the FXO gel prepared with a concentration of 0.01 mM of XO.

In order to determine if the artifact is visible at different doses, a set of 10 flasks containing the FXO gel was prepared. Subsequently, the Gammacell equipment was used to irradiate with doses ranging from 1 Gy to 10 Gy, with intervals of 1 Gy.

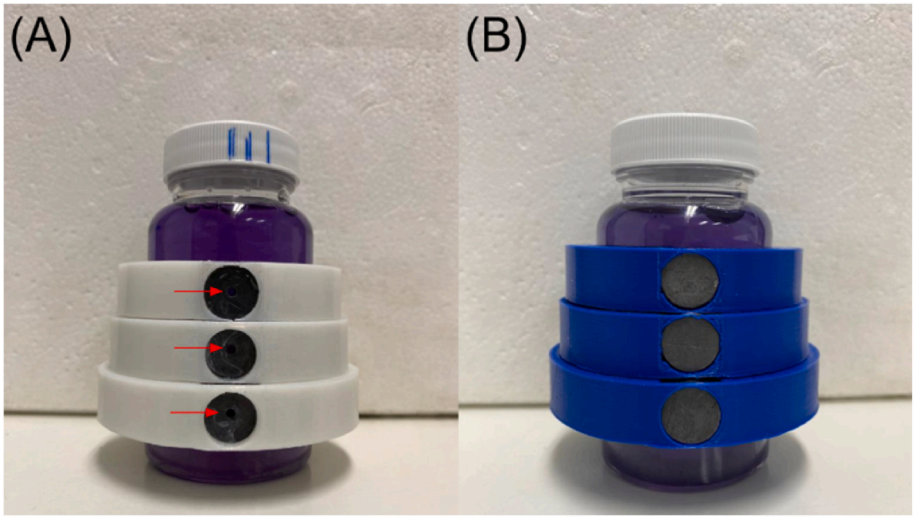

Fig. 5. The FXO gel flask irradiated configuration used in the experiment. A) with 5, 7, and 9 lead filters with a 0.1 mm central hole (pointed with red arrows); (B) with 5, 7, and 9 lead filters without a hole.

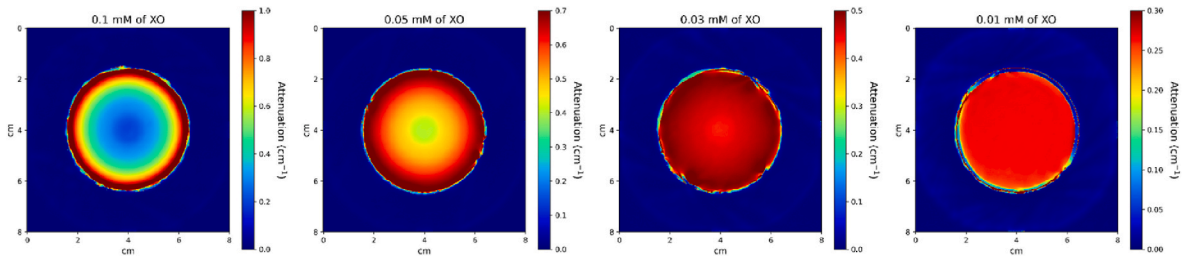

Fig. 6. Attenuation map for FXO gel irradiated with a Co-60 source at a dose of 10 Gy. Comparative visualization of different XO concentrations along the z-axis.

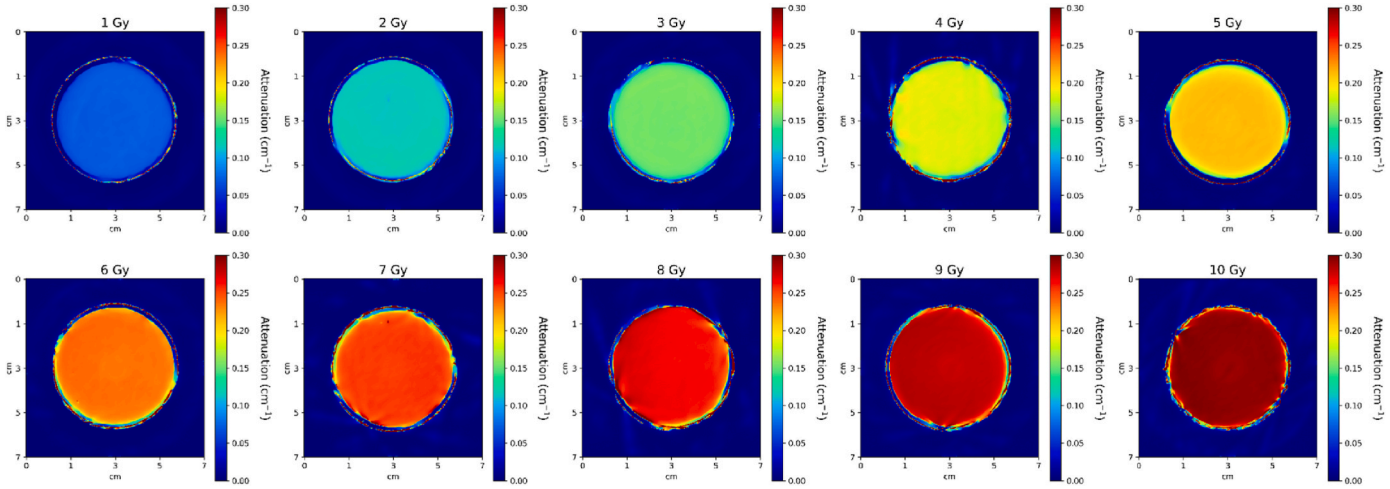

Fig. 7. Attenuation map for FXO gel with a 0.01 mM concentration of XO irradiated in a Gammacell irradiator in doses of 1 Gy–10 Gy in an interval of 1 Gy.

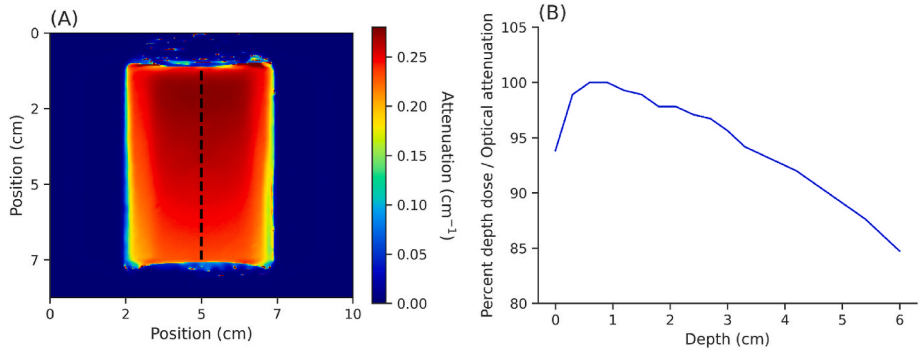

Fig. 8. (A) X-axis of a reconstructed image of FXO gel used for calibration in a Co-60 source. The black line represents the regions where points were used to obtain the PDD curve with a maximum dose delivered of 5 Gy, compared to a maximum attenuation value of 0.275 cm^{-1}. (B) Measured PDD at the central X-axis of FXO gel.

2.3. Calibration of Co-60 source in Theratron 780c irradiator

Theratron 780c is teletherapy equipment that utilizes a Co-60 source for irradiation applications. A water phantom measuring 30 cm × 30 cm x 20 cm was utilized to create a calibration curve using the FXO gel. The gel was placed into the phantom in a vertical orientation with a support. The apparatus utilized for this irradiation is illustrated in Fig. 4.

2.4. Irradiations in Theratron 780c irradiator for analysis in different regions of FXO gel

To conduct a comprehensive evaluation of attenuation in different areas after irradiation, the FXO gel was also irradiated in a teletherapy system with lead filters. The solution was irradiated with a 5 Gy dose from a Co-60 source in the Theratron 780c system while being in the water phantom of 30 cm × 30 cm x 20 cm. Fig. 2 illustrates the configuration of flaks for irradiation. Lead filters measuring 14 mm in diameter and 1 mm in thickness were employed in this configuration. To hold the filters, a holder was printed with 3D PLA material. Fig. 5A shows the first configuration with 5, 7, and 9 lead filters with a central hole of 0.1 mm diameter. Fig. 5B shows the second configuration with 5, 7, and 9 lead filters.

3. Results and discussion

3.1. Characterization of FXO gel for analysis in optical CT scanner Vista 16

The initial irradiation of this study aimed to determine the optimal concentration of XO for the gel in order to prevent any potential artifact issues. The results of gel reconstruction with doses of 0.1 mM, 0.05 mM, 0.03 mM, and 0.01 mM of XO are shown in Fig. 6.

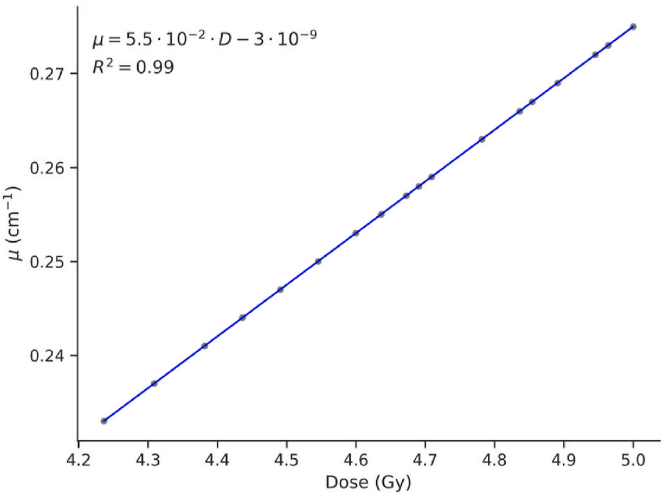

Fig. 9. Calibration curve of FXO gel irradiated with a Co-60 source in Theathron 780c equipment.

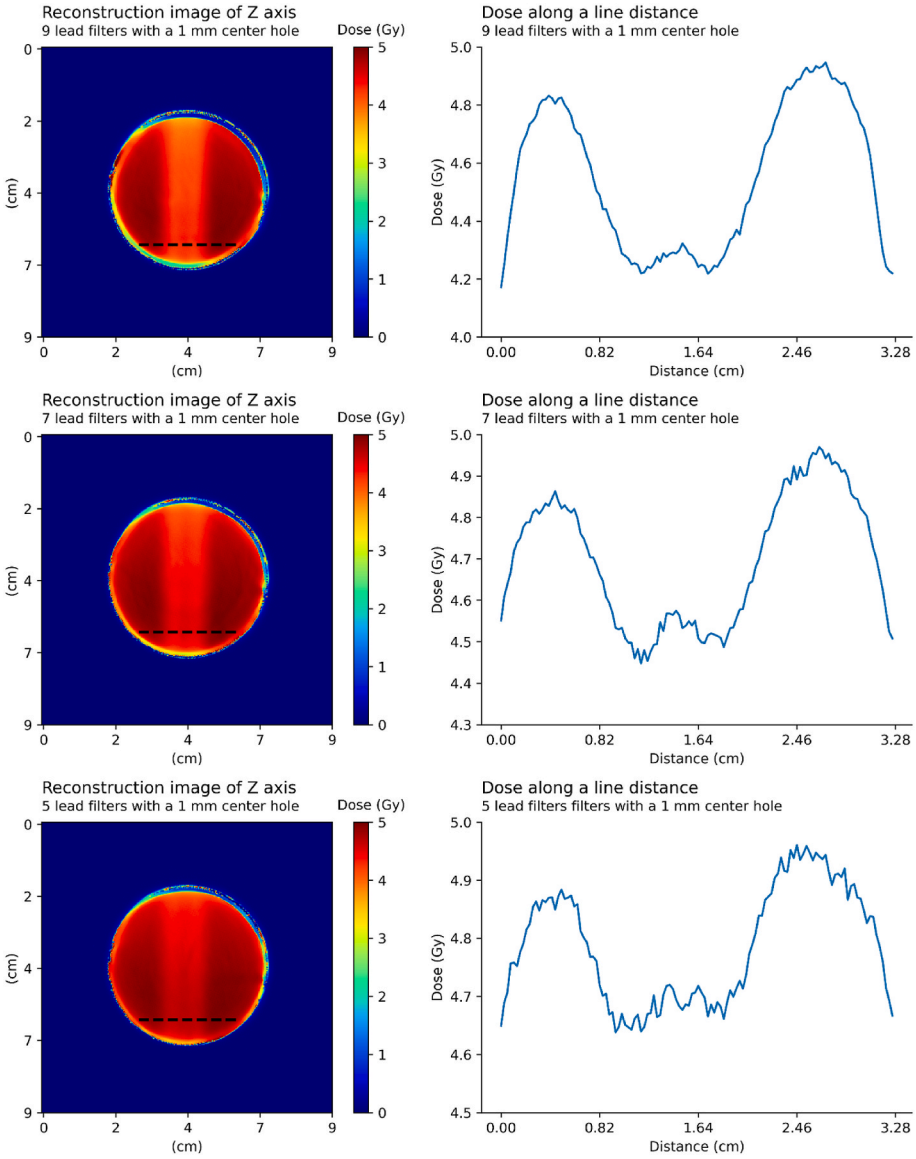

Fig. 10. Reconstruction images of Z-axis for the FXO gel irradiated with lead filters with a central hole and a graph illustrating dose along the distance of each lead shield region.

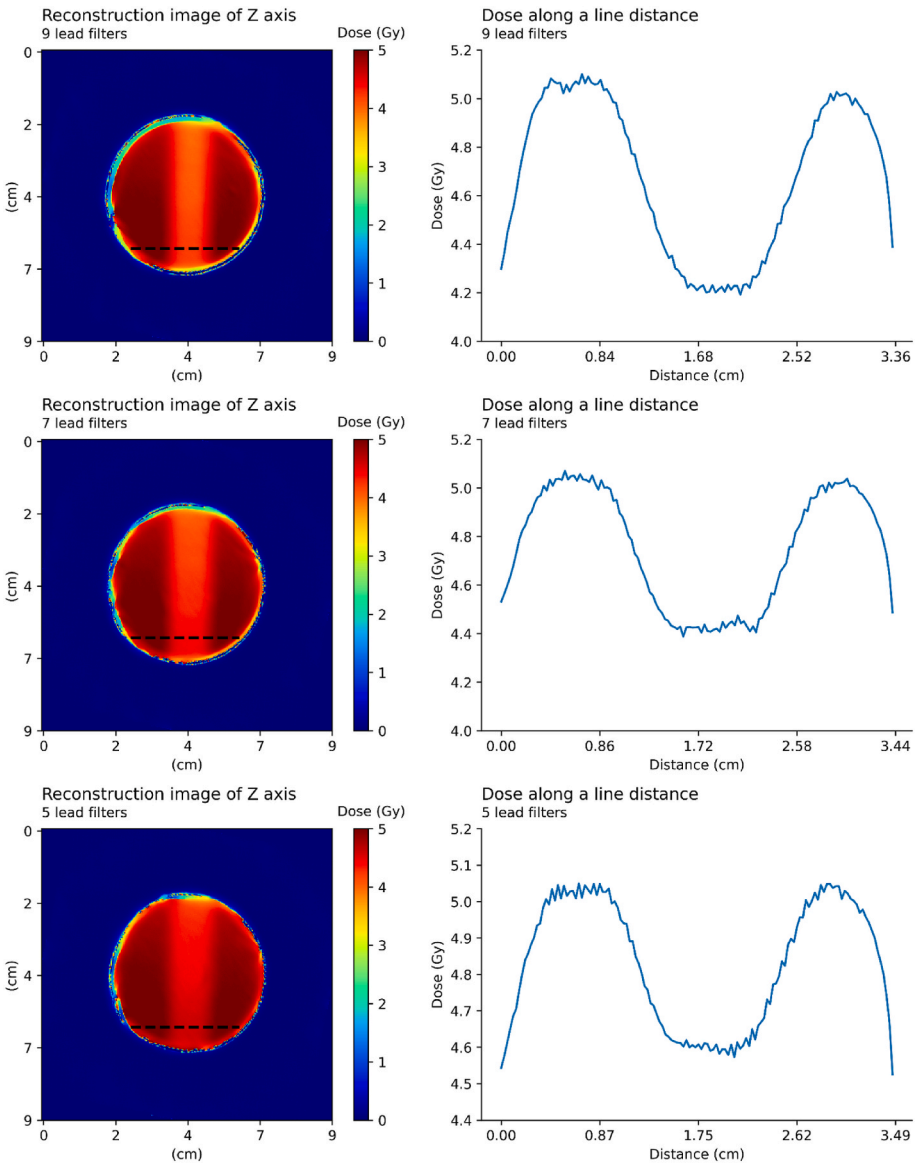

Fig. 11. Reconstruction images of Z-axis for the FXO gel irradiated with lead filters and a graph illustrating dose along the distance of each lead filters region.

The results shown in Fig. 6 illustrate the influence of XO concentration on the attenuation value. The colormap to the right of each reconstruction image displays a decrease in the correlation value with XO, which in consequence affects the presence of an artifact in the image. The existence of artifacts presents a challenge to the main purpose of the research, which is to validate doses in different regions within the FXO gel. As a result, the concentration of 0.01 mM does not exhibit any artifacts for this dose of 10 Gy.

A batch of 10 flasks containing FXO gel was prepared for irradiation in a Gammacell. The doses ranged from 1 Gy to 10 Gy, with an increment of 1 Gy. This enables the visualization of artifacts and the correlation between attenuation and dose. Fig. 7 displays the attenuation map for this experiment.

The results in Fig. 7 clearly demonstrate the correlation between attenuation and dose in this modified FXO gel for analysis. It enables the detection of artifacts within the dose range of 1 Gy–10 Gy.

3.2. Calibration curve in Theratron 780c irradiation

The reconstruction image in the x-axis obtained from the optical CT of the FXO gel sample irradiated with Theratron 780c provided a percent depth dose (PDD) (Fig. 8A). When comparing the maximum optical attenuation value at 5 Gy, it is observed that the maximum dose delivered corresponds to the PDD curve shown in Fig. 8B.

Fig. 9 illustrates a linear correlation between attenuation (μ) and absorbed dose. The linear behavior yields a sensitivity of $5.5{\cdot}10^{-3} \pm 2.6{\cdot}10^{-4}$ cm^{-1}/Gy and a correlation coefficient (R2) of 0.99. This linearity is used as a basis for creating a calibration curve and normalizing the dose distribution in order to compare measured and calculated images. The calibration curve for the attenuation coefficient begins at a dose of 4.2 Gy, which corresponds to 84% of the total dose.

3.3. Attenuation analysis in different regions of the FXO gel

The Z-axis, which represents the transverse plane, was chosen for analyzing each region where the lead filters were placed. Fig. 10 displays the reconstructed pictures of the Z-axis for the FXO hel irradiated with lead filters that have a central hole measuring 0.1 mm. Fig. 10 also contains a graph that demonstrates the dose at the distance of each lead shield region. The chosen line in the image is positioned adjacent to the edge of the flask, facing the beam, in order to capture the least amount of radiation attenuation induced by the gel volume.

While analyzing the reconstructed images, it is evident that there is a significant reduction in dose for each image with an increase in the quantity of lead filters. Regarding the 9 lead filters, the area that corresponds to the hole exhibits a considerable reduction in radiation dose, with a peak value of 4.32 Gy. This is evident in both the reconstruction and the graph. In the region with 7 lead filters, the peak in the center was measured to be 4.57 Gy. This indicates that the irradiation results in an increase of approximately 5.8% in dose between 7 and 9 lead filters. In the case of the 5 lead filters, the hole is indiscernible, and there is excessive noise in this area. Upon further analysis of the graph, it is evident that the maximum dose in the hole region was 4.72 Gy, which is approximately 9.2% greater than the dose in the hole of the 9 lead filters.

Fig. 11 shows the specific locations along the Z-axis where lead filters without holes were placed, indicating the transverse plane of the FXO gel. Fig. 11 includes a graph that shows the dose as it varies across the different regions of each lead filter. The analysis of the FXO gel with lead filters involves carefully positioning a selected line in the figure near the edge of the flask facing the beam. This position is chosen to capture the minimal attenuation produced by the gel volume.

While analyzing Fig. 11, it is evident that the region including 9 lead filters exhibits an average dose of 4.22 Gy. In the specific region with 7 lead filters, the average dose is around 4.43 Gy, which is approximately 4.9% greater than the dose with 9 lead filters. As a result, the average dose in the region with 5 lead filters is 4.61 Gy, which is 9.2% greater than the average dose with 9 lead filters.

4. Conclusions

The Optical CT Vista 16 is equipment for 3D dosimetry through the study of FXO gel. In order to prevent artifacts, it was necessary to assess the attenuation throughout the entire region for a modified FXO gel. In order to do this, it was necessary to introduce a variation of XO in the preparation. After utilizing a Gammacell system to irradiate the FXO gel, it was determined that the ideal concentration of XO is 0.01 mM in order to prevent any distortions within the dose range of 1 Gy–10 Gy.

A calibration system utilizing FXO gel can be developed by comparing the maximum irradiation dose with the attenuation observed in the gel. The modified gel exhibited a sensitivity of $5.5{\cdot}10^{-3} \pm 2.6{\cdot}10^{-4}$ cm^{-1}/Gy and a starting dose of 4.2 Gy.

To analyze regions of a gel, attempt to replicate a planning application. It utilized lead filters with a thickness of 1 mm. Two samples were tested using a configuration of 5, 7, and 9 lead filters. The initial samples were equipped with lead filters featuring a central hole. The central holes exhibit dose peaks of 4.72 Gy, 4.57 Gy, and 4.32 Gy, respectively.

In the second example, lead filters without perforations were utilized. Showed average doses of 4.22 Gy, 4.43 Gy, and 4.61 Gy for 9, 7, and 5 lead filters. The results indicate the feasibility of producing modified Fricke xylenol orange gels for examination in an optical CT system and their potential application in radiotherapy systems. Upcoming research is being conducted in the field of clinical irradiation to facilitate the comparison with system designs.

CRediT authorship contribution statement

P.V.S. Tavares: Writing – original draft, Software, Methodology, Investigation, Formal analysis, Data curation. **R.E. Diniz:** Methodology. **O. Rodrigues:** Supervision, Resources, Methodology, Investigation. **L.L. Campos:** Writing – review & editing, Supervision, Investigation.

Declaration of competing interest

The authors declare the following financial interests/personal relationships which may be considered as potential competing interests:

Leticia Lucente Campos reports financial support was provided by State of Sao Paulo Research Foundation. Paulo dos Santos Tavares reports financial support was provided by Brazilian Nuclear Energy Commission. If there are other authors, they declare that they have no known competing financial interests or personal relationships that could have appeared to influence the work reported in this paper.

Data availability

Data will be made available on request.

Acknowledgement

Acknowledgments to the funding agencies FAPESP under process number 2017/50332-0, CNPq under process number 426513/2018-5, CAPES under process number 88887.704665/2022-00, and CNEN for providing a scholarship. The Center of Technology Radiation is providing access to the Gammacell 600c for irradiation. The Calibration Instrument Laboratory for the use of Theatron 780c. These laboratories are located at the Institute of Nuclear Energy Research.

References

Al Kafi, M.A., Arib, M., Al Moussa, A., Alzorkany, F., Shehadeh, M., Mohd Yusof, M.F., Moftah, B., 2023. Small field output factor measurement and verification for CyberKnife robotic radiotherapy and radiosurgery system using 3D polymer gel, ionization chamber, diode, diamond and scintillator detectors, Gafchromic film and Monte Carlo simulation. Appl. Radiat. Isot. 192, 110576 https://doi.org/10.1016/j.apradiso.2022.110576.

Azadeh, P., Amiri, S., Mostaar, A., Yaghobi Joybari, A., Paydar, R., 2022. Evaluation of MAGIC-f polymer gel dosimeter for dose profile measurement in small fields and stereotactic irradiation. Radiat. Phys. Chem. 194, 109991 https://doi.org/10.1016/j.radphyschem.2022.109991.

Babu, S.E.S., Peace, B.S.T., Rafic, K.M., Raj, E.W.M., Christopher, J.S., Ravindran, B.P., 2019. Escalation of optical transmittance and determination of diffusion co-efficient in low-bloom strength gelatin-based Fricke gel dosimeters. Radiat. Phys. Chem. 156, 300–306. https://doi.org/10.1016/j.radphyschem.2018.10.001.

Bero, M.A., Gilboy, W.B., Glover, P.M., Keddie, J.L., 1999. Three-dimensional radiation dose measurements with Ferrous Benzoic Acid Xylenol Orange in Gelatin gel and optical absorption tomography. Nucl. Instrum. Methods Phys. Res. Sect. Accel. Spectrometers Detect. Assoc. Equip. 422, 617–620. https://doi.org/10.1016/S0168-9002(98)00970-X.

Bolten, J.-H., Dunst, J., Siebert, F.-A., 2023. Geometric accuracy in patient positioning for stereotactic radiotherapy of intracranial tumors. Phys. Imaging Radiat. Oncol. 27 https://doi.org/10.1016/j.phro.2023.100461.

Colins, K., Liu, Y., Li, L., Birdee, K., 2018. Radiation-induced damage-based system and method for indirectly monitoring high-dose ionizing radiation. Nucl. Technol. 201, 113–121. https://doi.org/10.1080/00295450.2017.1411718.

Dekker, K.H., Battista, J.J., Jordan, K.J., 2017. Technical Note: evaluation of an iterative reconstruction algorithm for optical CT radiation dosimetry. Med. Phys. 44, 6678–6689. https://doi.org/10.1002/mp.12635.

Del Lama, L.S., Petchevist, P.C.D., de Almeida, A., 2017. Fricke Xylenol Gel characterization at megavoltage radiation energy. Nucl. Instrum. Methods Phys. Res. Sect. B Beam Interact. Mater. Atoms 394, 89–96. https://doi.org/10.1016/j.nimb.2016.12.045.

Doran, S.J., Koerkamp, K.K., Bero, M.A., Jenneson, P., Morton, E.J., Gilboy, W.B., 2001. A CCD-based optical CT scanner for high-resolution 3D imaging of radiation dose distributions: equipment specifications, optical simulations and preliminary results. Phys. Med. Biol. 46, 3191–3213. https://doi.org/10.1088/0031-9155/46/12/309.

Gambarini, G., Arrigoni, S., Cantone, M.C., Molho, N., Facchielli, L., Sichirollo, A.E., 1994. Dose-response curve slope improvement and result reproducibility of ferrous-sulphate-doped gels analysed by NMR imaging. Phys. Med. Biol. 39, 703. https://doi.org/10.1088/0031-9155/39/4/004.

Gore, J.C., Kang, Y.S., 1984. Measurement of radiation dose distributions by nuclear magnetic resonance (NMR) imaging. Phys. Med. Biol. 29, 1189. https://doi.org/10.1088/0031-9155/29/10/002.

Gupta, B.L., Kini, U.R., Bhat, R.M., Madhvanath, U., 1982. Use of the FBX dosemeter for the calibration of cobalt-60 and high-energy teletherapy machines. Phys. Med. Biol. 27, 235–245. https://doi.org/10.1088/0031-9155/27/2/005.

Hayashi, K., Gotoh, H., 2020. Prediction of the presence of cupping artifacts for gel dosimeter based on considerations of scattered light in optical computed tomography measurements. Radiat. Meas. 138 https://doi.org/10.1016/j.radmeas.2020.106437.

Hefne, J., 2000. The dose distribution inside the irradiation chamber of the gamma cell 220 at KACST using MCNP4B. J. Nucl. Sci. Technol. 37, 402–405. https://doi.org/10.1080/00223131.2000.10874915.

Höfel, S., Liebig, P., Fix, M.K., Drescher, M., Zwicker, F., 2023. Adapting a practical EPR dosimetry protocol to measure output factors in small fields with alanine. J. Appl. Clin. Med. Phys. 24, e14191 https://doi.org/10.1002/acm2.14191.

Kelly, R.G., Jordan, K.J., Battista, J.J., 1998. Optical CT reconstruction of 3D dose distributions using the ferrous–benzoic–xylenol (FBX) gel dosimeter. Med. Phys. 25, 1741–1750. https://doi.org/10.1118/1.598356.

Liosi, G.M., Dondi, D., Vander Griend, D.A., Lazzaroni, S., D'Agostino, G., Mariani, M., 2017. Fricke-gel dosimeter: overview of Xylenol Orange chemical behavior. In: Radiat. Phys. Chem., 2nd International Conference on Dosimetry and its Applications (ICDA-2) University of Surrey. Guildford, United Kingdom, pp. 74–77. https://doi.org/10.1016/j.radphyschem.2017.01.012.

Luciani, A.M., Capua, S.D., Guidoni, L., Ragona, R., Rosi, A., Viti, V., 1996. Multiexponential relaxation in Fricke agarose gels: implications for NMR dosimetry. Phys. Med. Biol. 41, 509. https://doi.org/10.1088/0031-9155/41/3/012.

Matenine, D., Goussard, Y., Després, P., 2015a. GPU-accelerated regularized iterative reconstruction for few-view cone beam CT. Med. Phys. 42, 1505–1517. https://doi.org/10.1118/1.4914143.

Matenine, D., Mascolo-Fortin, J., Goussard, Y., Després, P., 2015b. Evaluation of the OSC-TV iterative reconstruction algorithm for cone-beam optical CT. Med. Phys. 42, 6376–6386. https://doi.org/10.1118/1.4931604.

Mendes, Karla Ferreira, Mendes, Kassio Ferreira, Guedes, S.F., Silva, L.C.A.S., Arthur, V., 2020. Evaluation of physicochemical characteristics in cherry tomatoes irradiated with 60Co gamma-rays on post-harvest conservation. Radiat. Phys. Chem. 177, 109139 https://doi.org/10.1016/j.radphyschem.2020.109139.

Moradi, F., Khandaker, M.U., Abdul Sani, S.F., Uguru, E.H., Sulieman, A., Bradley, D.A., 2021. Feasibility study of a minibeam collimator design for a 60Co gamma irradiator. Radiat. Phys. Chem., The 2nd International Forum on Advances in Radiation Physics (IFARP-2) 178, 109026. https://doi.org/10.1016/j.radphyschem.2020.109026.

Oldham, M., Siewerdsen, J.H., Kumar, S., Wong, J., Jaffray, D.A., 2003. Optical-CT gel-dosimetry I: basic investigations. Med. Phys. 30, 623–634. https://doi.org/10.1118/1.1559835.

Olding, T., Holmes, O., Schreiner, L.J., 2009. Scatter corrections for cone beam optical CT. J. Phys. Conf. Ser. 164 https://doi.org/10.1088/1742-6596/164/1/012031.

Potetnya, V.I., Koryakina, E.V., Troshina, M.V., Koryakin, S.N., 2021. Use of the chemical Fricke dosimeter and its modifications for dosimetry of gamma neutron radiation of a pulsed reactor. Nucl. Energy Technol. 7, 231–237. https://doi.org/10.3897/nucet.7.74149.

Rodrigues, R.R., Grynberg, S.E., Ferreira, A.V., Belo, L.C.M., Squair, P.L., Sousa, R.V., Sebastião, R.C.O., Ribeiro, M.A., 2010. Retrieval of GammaCell 220 irradiator isodose curves with MCNP simulations and experimental measurements. Braz. J. Phys. 40, 120–124. https://doi.org/10.1590/S0103-97332010000100017.

Rousseau, A., Stien, C., Bordy, J.-M., Blideanu, V., 2022. Fricke-Xylenol orange-Gelatin gel characterization with dual wavelength cone-beam optical CT scanner for applications in stereotactic and dynamic radiotherapy. Phys. Med. 97, 1–12. https://doi.org/10.1016/j.ejmp.2022.03.008.

Rousseau, A., Stien, C., Gouriou, J., Bordy, J.-M., Boissonnat, G., Chabert, I., Dufreneix, S., Blideanu, V., 2023. End-to-end quality assurance for stereotactic radiotherapy with Fricke-Xylenol orange-Gelatin gel dosimeter and dual-wavelength cone-beam optical CT readout. Phys. Med. 113, 102656 https://doi.org/10.1016/j.ejmp.2023.102656.

Takanashi, T., Hayashi, K., Nemoto, M., Kawamura, H., Hayashi, S.-I., Gotoh, H., 2019. Cause of cupping artifacts from radiochromic micelle gel dosimeters used in optical CT scanner measurement. J. Phys. Conf. Ser. 1305, 012020 https://doi.org/10.1088/1742-6596/1305/1/012020.

Woolvett, N., Jordan, K., 2023. Modified optical computed tomography scanner for low temperature scanning. In: Presented at the Journal of Physics: Conference Series. https://doi.org/10.1088/1742-6596/2630/1/012020.

Xu, Y., Wuu, C.-S., Maryanski, M.J., 2004. Performance of a commercial optical CT scanner and polymer gel dosimeters for 3-D dose verification. Med. Phys. 31, 3024–3033. https://doi.org/10.1118/1.1803674.